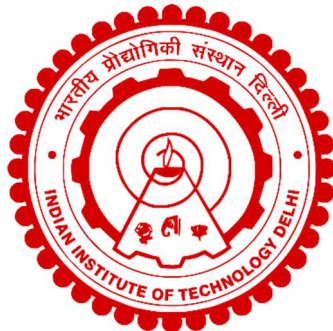


CHARACTERIZATION OF BACKFIRE AND POSTFIRE IN A HYDROGEN FUELLED SPARK IGNITION ENGINE

AKSHEY MARWAHA



Department of Energy Science and Engineering
INDIAN INSTITUTE OF TECHNOLOGY DELHI

MAY 2024

© Indian Institute of Technology Delhi (IITD), New Delhi, 2024

**CHARACTERIZATION OF BACKFIRE AND
POSTFIRE IN A HYDROGEN FUELLED SPARK
IGNITION ENGINE**

by

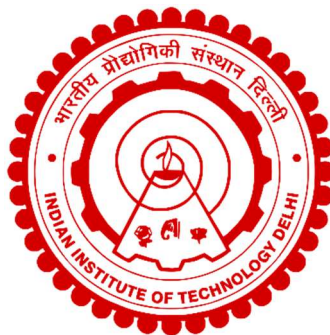
AKSHEY MARWAHA

Department of Energy Science and Engineering

Submitted

in fulfillment of the requirements of the degree of Doctor of Philosophy

to the



INDIAN INSTITUTE OF TECHNOLOGY DELHI

MAY 2024

Certificate

This is to certify that the thesis entitled “**Characterization of Backfire and Postfire in a Hydrogen fuelled Spark Ignition Engine**”, being submitted by **Akshey Marwaha** to the **Indian Institute of Technology Delhi** for the award of the degree of Doctor of Philosophy is a record of the bonafide research carried out by him which has been prepared under my supervision in conformity with the rules and regulations of the Indian Institute of Technology Delhi. He has fulfilled all requirements for the submission of his thesis, which has attained the standard required for a Ph.D. degree of the Institute. The research reports and results presented in the thesis have not been submitted for any degree in any other university or institute.

Place: New Delhi

Date:

Prof. K.A. Subramanian
Professor
Department of Energy Science and Engineering
Indian Institute of Technology Delhi
New Delhi – 110016
India

Acknowledgements

I am very grateful to my supervisor, Prof. K.A. Subramanian for providing me the opportunity to carry out Ph.D. research work under his guidance. He provided me with the best possible support and guidance needed for my research work. The in-depth discussions with him helped me to develop a research mindset and the ability to critically analyze the data. He constantly motivated me to become better and provided me with the necessary suggestions for the same. He provided me with all the advanced research facilities in the laboratory needed for my research work. I will be forever grateful to him.

I would like to thank my SRC members Prof. Kaushik Saha (Internal member, DESE), Prof. S.K. Tyagi (Chairman, SRC) and Prof. Deepak Kumar (External member, SRC) for their valuable inputs and constant encouragement for my research work.

I am thankful to Dr. Vipin Dhyani for providing me with the necessary support and knowledge about the operation of hydrogen engine during the starting of my Ph.D. journey. I am also thankful to my senior lab members - Dr. Sachin Gupta, Dr. Nidhi and Dr. Anilkumar Shere for sharing their valuable inputs and suggestions in the research.

I would like to thank Mr. Divyanshu for assisting me during the experiments. I would also like to thank Mr. Rohan Kumar, Mr. Rajneesh Kashyap, Mr. Anurag Gaur and Mr. Akhil Ailaboina for their help during the experiments. I am thankful to Mr. Ashutosh Kumar (Senior Lab Assistant, Engines and Unconventional Fuels Laboratory) for helping me with the purchase of different engine accessories needed during the experiments.

Lastly, I am forever grateful to my parents, Dr. Sanjay Marwaha and Dr. Anupma Marwaha for their constant support, encouragement and blessings. They have always motivated me to do better in life and given me endless support whenever I needed it. I am forever grateful to them.

Place: New Delhi

Date:

(Akshey Marwaha)

Abstract

Backfire is an abnormal combustion phenomenon occurring during the suction stroke of a manifold hydrogen injection-based spark ignition engine due to mainly external ignition sources including residual gas temperature, hot spots, partially burned lubricating oil, hot engine components, misfire and postfire. Backfire results in an audible high-pitched sound with speed drop, decrease in mean effective pressure, stalling the engine operation, and damaging of engine components. This present work is aimed at investigation of backfire occurrence and its propagation in an automotive spark ignition engine fuelled with hydrogen.

A gasoline automotive four-stroke spark ignition engine (15 kW) was modified to a hydrogen engine by incorporating mainly a timed manifold hydrogen injection system. A transparent intake manifold system was developed and attached to the engine to visualize the propagation of backfire. A high-speed camera was used to capture the real-time backfire images during the engine running. The engine was run with varied speeds and torque. The experimental results indicate that backfire occurrence probability increases with the increase in torque at constant speed, the increase in speed (at constant torque), high equivalence ratio and the increase in torque with the decrease in speed (at constant brake power).

It is practically observed that the residual (exhaust) gas temperature plays a critical role in acting as one of the external ignition sources to initiate backfire when a fresh air-hydrogen mixture interacts with the residual gas inside the cylinder during the engine's suction stroke. The critical exhaust gas temperatures (EGT) identified for the backfire initiation are in the range of 765 °C to 955 °C for speeds from 2000 rpm to 4900 rpm. A dimensionless backfire occurrence number (BON) was developed using the experimental results to predict backfire occurrence, where BON

greater than or equal to zero denotes backfire occurrence. Backfire occurrence is strongly linked to other abnormal combustion phenomena called misfire and postfire.

Misfire occurs during engine cranking due to too low spark duration, low in-cylinder temperature, fouled spark plug and too much advanced spark timing and the accumulation of the unburnt hydrogen during misfire burns in subsequent cycle leading to Postfire occurrence during exhaust stroke resulting in backfire. The Indicated Mean Effective Pressure based coefficient of variation during backfire, postfire and misfire was above 5% resulting in combustion instability of the engine. The CFD results indicate about 13% unburnt hydrogen as a scavenging loss leaves the exhaust manifold during the misfire cycle and the charge temperature is in the range of 1300 to 1500 K near the intake valve during backfire propagation. The pressure rise in the exhaust manifold during postfire was observed beyond 2 bar. The backfire is characterized using backfire ignition delay, expansion, convergence and termination. The average backfire propagation velocity calculated using high-speed camera images is found to be 179.3 m/s corresponding to a Mach number of 0.52 at an equivalence ratio of 0.5 and hence, backfire under varied engine speed can be characterized as deflagration (subsonic). Simultaneous acquiring of the intake manifold and in-cylinder pressure was found a reliable approach for estimating backfire propagation velocity.

The notable findings that emerged from the study are that backfire is strongly linked with misfire and postfire occurrence. The probability of backfire could be reduced by retardation of hydrogen injection timing, optimization of spark timing, high reactant velocity, and elimination of misfire and postfire.

सार

बैकफायर एक असामान्य दहन घटना है जो मैनिफोल्ड हाइड्रोजन इंजेक्शन-आधारित स्पार्क इग्निशन इंजन के सक्शन स्ट्रोक के दौरान मुख्य रूप से बाहरी इग्निशन स्रोतों के कारण होती है, जिसमें अवशिष्ट गैस तापमान, हॉट स्पॉट, आंशिक रूप से जला हुआ चिकनाई तेल, गर्म इंजन घटक, मिसफायर और पोस्टफायर शामिल हैं। बैकफायर के परिणामस्वरूप गति में गिरावट, औसत प्रभावी दबाव में कमी, इंजन संचालन में रुकावट और इंजन घटकों को नुकसान के साथ उच्च-तीक्ष्ण ध्वनि सुनाई देती है। इस वर्तमान कार्य का उद्देश्य हाइड्रोजन से संचालित ऑटोमोटिव स्पार्क इग्निशन इंजन में बैकफायर घटना और इसके प्रसार की जांच करना है।

एक गैसोलीन ऑटोमोटिव फोर-स्ट्रोक स्पार्क इग्निशन इंजन (15 किलोवाट) को मुख्य रूप से टाइम्ड मैनिफोल्ड हाइड्रोजन इंजेक्शन प्रणाली को शामिल करके हाइड्रोजन इंजन में संशोधित किया गया था। बैकफायर के प्रसार को देखने के लिए एक पारदर्शी इनटेक मैनिफोल्ड सिस्टम विकसित किया गया और इंजन से जोड़ा गया। इंजन चलने के दौरान वास्तविक समय की बैकफायर छवियों को कैच करने के लिए एक हाई-स्पीड कैमरे का उपयोग किया गया था। इंजन को विभिन्न गति और टॉर्क के साथ चलाया गया। प्रयोगात्मक परिणामों से संकेत मिलता है कि स्थिर गति पर टॉर्क में वृद्धि, गति में वृद्धि (स्थिर टॉर्क पर), उच्च तुल्यता अनुपात और गति में कमी (निरंतर ब्रेक पावर पर) के साथ टॉर्क में वृद्धि के साथ बैकफायर घटना की संभावना बढ़ जाती है।

यह व्यावहारिक रूप से देखा गया है कि जब ताजी हवा-हाइड्रोजन मिश्रण इंजन के सक्शन स्ट्रोक के दौरान सिलेंडर के अंदर अवशिष्ट गैस के साथ संपर्क करता है, तो अवशिष्ट (निकास) गैस का तापमान बैकफायर शुरू करने के लिए बाहरी इग्निशन स्रोतों में से एक के रूप में कार्य करने में महत्वपूर्ण भूमिका निभाता है। बैकफायर आरंभ के लिए पहचाने जाने वाले महत्वपूर्ण निकास गैस तापमान (ईजीटी) 2000 आरपीएम से

4900 आरपीएम तक की गति के लिए 765 डिग्री सेल्सियस से 955 डिग्री सेल्सियस की सीमा में हैं। बैकफ़ायर घटना की भविष्यवाणी करने के लिए प्रयोगात्मक परिणामों का उपयोग करके एक आयाम रहित बैकफ़ायर घटना संख्या (बीओएन) विकसित किया गया था, जहां शून्य से अधिक या उसके बराबर बीओएन बैकफ़ायर घटना को दर्शाता है। बैकफ़ायर की घटना अन्य असामान्य दहन घटनाओं से दृढ़ता से जुड़ी हुई है जिन्हें मिसफ़ायर और पोस्टफ़ायर कहा जाता है।

बहुत कम स्पार्क अवधि, कम इन-सिलेंडर तापमान, खराब स्पार्क प्लग और बहुत अधिक उन्नत स्पार्क टाइमिंग के कारण इंजन क्रैंकिंग के दौरान मिसफ़ायर होता है और बाद के चक्र में मिसफ़ायर जलने के दौरान बिना जले हाइड्रोजन का संचय होता है, जिससे एग्जॉस्ट स्ट्रोक के दौरान पोस्टफ़ायर की घटना होती है, जिसके परिणामस्वरूप बैकफ़ायर होता है। . बैकफ़ायर, पोस्टफ़ायर और मिसफ़ायर के दौरान भिन्नता का संकेतित औसत प्रभावी दबाव आधारित गुणांक 5% से ऊपर था जिसके परिणामस्वरूप इंजन की दहन अस्थिरता हुई। सीएफडी परिणामों से संकेत मिलता है कि मिसफ़ायर चक्र के दौरान निकास में होने वाली हानि के कारण लगभग 13% अधजला हाइड्रोजन निकलता है और बैकफ़ायर प्रसार के दौरान इनटेक वाल्व के पास चार्ज तापमान 1300 से 1500 K की सीमा में होता है। पोस्टफ़ायर के दौरान एग्जॉस्ट मैनिफोल्ड में दबाव 2 बार से अधिक बढ़ गया। बैकफ़ायर को बैकफ़ायर इग्निशन विलंब, विस्तार, अभिसरण और समाप्ति का उपयोग करके चित्रित किया गया है। हाई-स्पीड कैमरा छवियों का उपयोग करके गणना की गई औसत बैकफ़ायर प्रसार वेग 0.5 के समतुल्य अनुपात पर 0.52 की मच संख्या के अनुरूप 179.3 मीटर/सेकेंड पाया गया है और इसलिए, विभिन्न इंजन गति के तहत बैकफ़ायर को अपस्फीति (सबसोनिक) के रूप में वर्णित किया जा सकता है। इनटेक मैनिफोल्ड और इन-सिलेंडर दबाव को एक साथ प्राप्त करने से बैकफ़ायर प्रसार वेग का अनुमान लगाने के लिए एक विश्वसनीय दृष्टिकोण पाया गया।

अध्ययन से जो उल्लेखनीय निष्कर्ष सामने आए, वे यह हैं कि बैकफ़ायर का मिसफ़ायर और पोस्टफ़ायर घटना से गहरा संबंध है। हाइड्रोजन इंजेक्शन समय की मंदता, स्पार्क टाइमिंग का अनुकूलन, उच्च प्रतिक्रियाशील वेग, और मिसफ़ायर और पोस्टफ़ायर को खत्म करके बैकफ़ायर की संभावना को कम किया जा सकता है।

Table of Contents

Certificate.....	i
Acknowledgements.....	ii
Abstract.....	iv
Table of Contents.....	ix
List of Figures.....	xv
List of Tables.....	xxi
Nomenclatures.....	xxii
Chapter 1: Introduction.....	1
1.1 Global scenario of energy and emissions.....	1
1.2 Hydrogen for decarbonization of various sectors.....	2
1.2.1 Hydrogen production and storage.....	5
1.2.2 Hydrogen utilization in internal combustion engines.....	6
1.3 Present research work and adopted approach.....	8
Chapter 2: Literature Review.....	10
2.1 Abnormal combustion occurrence in hydrogen fuelled SI engines.....	10
2.1.1 Backfire occurrence in hydrogen fuelled SI engines.....	12
2.1.2 Interlink among the occurrence of abnormal combustion phenomena.....	14
2.1.3 Closure.....	15

2.2 Identification and characterization of abnormal combustion phenomenon.....	16
2.2.1 Identification of misfire.....	16
2.2.2 Identification and characterization of knocking.....	18
2.2.3 Identification and characterization of backfire occurrence and propagation.....	20
2.2.4 Closure.....	20
2.3 Control of backfire occurrence	21
2.3.1 Closure.....	23
2.4 Research Gaps.....	24
Chapter 3: Objectives, Methodology, Experimental and model details.....	25
3.1 Objectives.....	25
3.2 Methodology.....	25
3.2.1 Distinction of abnormal combustion events using pressure signals.....	27
3.2.1.1 Misfire occurrence.....	28
3.2.1.2 Postfire occurrence.....	28
3.2.1.3 Backfire occurrence.....	28
3.2.2 Combustion and performance characteristics.....	28
3.2.2.1 Uncertainty calculation.....	33
3.2.3 Engine geometry preparation and case setup for CFD analysis.....	35

3.2.3.1 Case setup for misfire cycle.....	37
3.2.4 Numerical calculations.....	37
3.2.4.1 Calculation of localized equivalence ratio.....	38
3.2.4.2 Calculation of reaction time.....	39
3.2.4.3 Calculation of induction time using global one-step reaction.....	39
3.2.4.4 Calculation of conversion time from HO ₂ to OH radical using detailed chemical reaction mechanism.....	40
3.2.5 Backfire propagation.....	41
3.2.5.1 Laminar burning velocity.....	41
3.2.5.2 Turbulent backfire propagation.....	41
3.2.5.2.1 High speed camera images.....	41
3.2.5.2.2 Simultaneous acquisition of intake manifold and in-cylinder pressure signals...	43
3.2.5.2.3 CFD simulation case setup for normal combustion and backfire.....	44
3.2.5.2.4 Engine stalling mechanism due to backfire propagation.....	44
3.2.5.2.5 Forced air induction to suppress backfire propagation.....	44
3.3 Experimental and model details.....	45
3.3.1 Experimental test setup details.....	46
3.3.2 Computational setup and model details.....	50
Chapter 4: Results and Discussion.....	53

4.1 Backfire occurrence in hydrogen fuelled automotive SI engine.....	53
4.1.1 Effect of operating parameters on backfire.....	53
4.1.1.1 Effect of hydrogen injection timing on backfire occurrence.....	53
4.1.1.2 Effect of varying torque at constant engine speed on backfire occurrence.....	54
4.1.1.3 Effect of varying engine speed at constant torque on backfire occurrence.....	56
4.1.1.4 Effect of varying speed and torque at constant brake power on backfire occurrence.....	60
4.1.1.5 Effect of varying equivalence ratio at constant speed on backfire occurrence.....	62
4.1.1.6 Backfire limiting equivalence ratio at different engine speeds.....	62
4.1.1.6.1 Effect of reaction time on backfire occurrence.....	68
4.1.1.6.1.1 Chemical reaction mechanism analysis.....	70
4.1.1.7 Effect of engine speed and spark timing on backfire occurrence.....	73
4.1.1.7.1 Spark timing optimization for stable combustion and higher IMEP without backfire occurrence.....	74
4.1.1.7.2 Net IMEP at different engine speeds without backfire occurrence.....	77
4.1.1.8 Prediction of backfire occurrence (Backfire occurrence number).....	79
4.1.1.9 Backfire occurrence due to misfire and postfire.....	79

4.1.1.9.1 Effect of misfire and postfire on backfire occurrence during engine cranking.....	79
4.1.1.9.2 Effect of misfire and postfire on backfire occurrence during engine running.....	81
4.1.1.9.3 Misfire occurrence due to too low spark duration.....	86
4.1.1.9.4 Characterization of postfire.....	86
4.1.2 Association of backfire occurrence with engine speed.....	88
4.1.3 Closure.....	90
4.2 Backfire propagation in hydrogen fuelled automotive SI engine.....	91
4.2.1 Mechanism of backfire propagation.....	91
4.2.2 Characterization of backfire propagation.....	93
4.2.2.1 High speed camera images.....	93
4.2.2.2 Simultaneous acquisition of intake manifold and in-cylinder pressure signals.....	97
4.2.2.3 Interlink between backfire intensity and backfire propagation duration.....	100
4.2.3 CFD simulation.....	103
4.2.4 Effect of backfire propagation on engine stalling.....	111
4.2.5 Suppression of backfire propagation by forced air induction.....	116
4.2.6 Closure.....	118
4.3 Summary of Results.....	119

4.3.1 Novelty of the research work.....	121
Chapter 5: Conclusions and Future Works.....	123
5.1 Conclusions.....	123
5.1.1 Backfire occurrence.....	123
5.1.2 Backfire propagation.....	125
5.2 Future Works.....	127
References.....	128
Appendices.....	143
Appendix A. Simulation time parameters, Initialization conditions, and Boundary conditions.....	143
Appendix B. Technical specifications of sensor and instruments.....	146
List of publications and awards.....	157
Brief biodata of the author.....	160

List of Figures

Fig. 1.1 Flowchart of the carried research work.....	9
Fig. 3.1 Geometry preparation for CFD analysis.....	36
Fig. 3.2 Developed geometry with flagged boundaries.....	36
Fig. 3.3 In-cylinder pressure at different base grid sizes.....	37
Fig. 3.4 Intake valve profile.....	38
Fig. 3.5 a) Raw image with default settings b) Post-processed image with optimum settings.....	42
Fig. 3.6. Flowchart of the methodology adopted for research work.....	45
Fig. 3.7. Schematic layout of experimental setup.....	47
Fig. 3.8. Pictorial layout of experimental setup.....	48
Fig. 3.9. Close view of auxiliary setup between engine and transparent intake manifold.....	48
Fig. 4.1. Effect of hydrogen injection timing on backfire.....	54
Fig. 4.2. Time available for cooling of residual charge at 3000 rpm	55
Fig. 4.3. Effect of increasing torque at constant speed on in-cylinder pressure.....	55
Fig. 4.4. Effect of increasing torque at constant speed on COV IMEP.....	56
Fig. 4.5. Effect of increasing torque at constant speed on EGT, RGT, and backfire occurrence.....	57
Fig. 4.6. Effect of increasing speed at constant torque on in-cylinder pressure.....	58
Fig. 4.7. Effect of increasing speed at constant torque on EGT and backfire occurrence.....	58

Fig. 4.8. Effect of increasing speed at constant torque on net IMEP.....	59
Fig. 4.9. Effect of increasing speed at constant torque on COV IMEP.....	59
Fig. 4.10. Effect of varying speed and torque at constant brake power on in-cylinder pressure.....	60
Fig. 4.11. Effect of varying speed and torque on peak in-cylinder pressure and HRR.....	61
Fig. 4.12. Effect of varying speed and torque at constant brake power on backfire occurrence.....	61
Fig. 4.13. Effect of increasing equivalence ratio at constant brake power on backfire occurrence.....	62
Fig. 4.14. Exhaust gas temperature and BLER at different engine speeds.....	63
Fig. 4.15. Hydrogen and air mass flow profile with respect to crank angle.....	65
Fig. 4.16. Localized equivalence ratio.....	65
Fig. 4.17. In-cylinder pressure at different engine speeds.....	67
Fig. 4.18. Brake thermal efficiency and combustion duration at different engine speeds.....	67
Fig. 4.19. The link between reaction time and engine speed.....	69
Fig. 4.20. The link between critical EGT and reaction time.....	69
Fig. 4.21. Induction time with respect to reactant temperature and equivalence ratio.....	71
Fig. 4.22. Conversion time of HO ₂ to OH radical.....	72
Fig. 4.23. Variation of backfire limiting spark timing with engine speed.....	73
Fig. 4.24. In-cylinder pressure at varying spark timing.....	74
Fig. 4.25. Location of peak pressure at varying spark timing.....	75

Fig. 4.26. Net IMEP at varying spark timing.....	76
Fig. 4.27. COV IMEP at varying spark timing.....	76
Fig. 4.28. Brake thermal efficiency at varying spark timing.....	77
Fig. 4.29. Net IMEP at different engine speeds.....	78
Fig. 4.30. COV IMEP at different engine speeds.....	78
Fig. 4.31. a) Backfire occurrence due to misfire and postfire during engine cranking b) Close view of postfire occurrence c) Close view of backfire occurrence.....	80
Fig. 4.32. Effect of abnormal combustion on indicated mean effective pressure during engine cranking.....	81
Fig. 4.33. a) Misfire, postfire and backfire occurrence during engine running b) Close view of postfire occurrence c) Close view of backfire occurrence.....	82
Fig. 4.34. Effect of abnormal combustion on indicated mean effective pressure.....	84
Fig. 4.35. Validation of simulated in-cylinder pressure with experimental data during misfire....	85
Fig. 4.36. Simulated mass flow profile of hydrogen during a misfire cycle.....	85
Fig. 4.37. Spark duration during normal combustion and misfire.....	86
Fig. 4.38. Characteristics of postfire occurrence.....	87
Fig. 4.39. Backfire occurrence at high engine speeds.....	88
Fig. 4.40. Location of backfire occurrence on mass flow profile.....	89

Fig. 4.41. Time for consumption of hydrogen-air mixture by backfire near SOI and backfire near IVC.....	89
Fig. 4.42. LBV of hydrogen-air at different reactant pressure and equivalence ratio	92
Fig. 4.43. High speed camera images of backfire propagation.....	94
Fig. 4.44. Backfire propagation velocity and flame area with time.....	95
Fig. 4.45. Close view of backfire propagation.....	95
Fig. 4.46. Backfire expansion and convergence of its propagation.....	96
Fig. 4.47. Backfire propagation duration using simultaneous acquisition of pressure signals.....	97
Fig. 4.48. Simultaneous acquisition of pressure signals during normal combustion.....	99
Fig. 4.49. Simultaneous acquisition data with backfire propagation duration of 37°CA.....	100
Fig. 4.50. Simultaneous acquisition data with backfire propagation duration of 28°CA.....	101
Fig. 4.51. Simultaneous acquisition data with backfire propagation duration of 22°CA.....	101
Fig. 4.52. Simultaneous acquisition data with backfire propagation duration of 21°CA.....	102
Fig. 4.53. Simultaneous acquisition data with backfire propagation duration of 15°CA.....	102
Fig. 4.54. Link between backfire intensity and backfire propagation duration.....	103
Fig. 4.55. In-cylinder pressure validation of experimental data with simulation.....	104
Fig. 4.56. Temperature contour plots showing backfire origin near exhaust valve (CFD result)	105

Fig. 4.57. Increase in localized temperature near exhaust valve due to backfire origin (CFD result)	105
Fig. 4.58. Temperature contour plots showing backfire propagation towards intake valve (CFD result)	106
Fig. 4.59. High localized temperature near the intake valve (CFD result)	106
Fig. 4.60. Increase in in-cylinder pressure due to backfire occurrence during suction stroke (CFD result)	107
Fig. 4.61. Increase in HRR due to backfire occurrence during suction stroke (CFD result)	108
Fig. 4.62. Decrease in oxygen concentration due to backfire occurrence (CFD result)	108
Fig. 4.63. Decrease in nitrogen concentration due to backfire occurrence (CFD result)	109
Fig. 4.64. Increase in concentration of OH radical due to backfire occurrence (CFD result)	109
Fig. 4.65. Increase in concentration of HO ₂ radical due to backfire occurrence (CFD result)	110
Fig. 4.66. Increase in concentration of H ₂ O ₂ radical due to backfire occurrence (CFD result)	110
Fig. 4.67. Stalling due to backfire and without backfire	111

Fig. 4.68. Expanded profile of intake manifold pressure before, during and after backfire occurrence.....	112
Fig. 4.69. Intake manifold pressure of a) Cycles before backfire occurrence b) Backfire cycle c) Cycles after backfire occurrence.....	113
Fig. 4.70. a) Advancement of the location of abnormal combustion towards early suction stroke b) Crank angle location of abnormal combustion and engine speed variation with cycle number.....	114
Fig. 4.71. Dependence of engine stalling on backfire origin crank angle.....	115
Fig. 4.72. In-cylinder pressure with natural and forced air induction.....	116
Fig. 4.73. a) PMEP and b) Net IMEP with natural and forced air induction.....	117
Fig. 4.74. Combustion stability with natural and forced air induction.....	117
Fig. 4.75. High speed camera image a) Natural b) Forced air induction.....	118

List of Tables

Table 1.1 National hydrogen roadmaps and strategies.....	3
Table 3.1 Uncertainty in measured and calculated parameters.....	35
Table 3.2 Comparison of detailed mechanisms.....	40
Table 3.3 Optimum settings in PCC software for better visualization of backfire propagation.....	42
Table 3.4 Technical specifications of the engine.....	46
Table 3.5 Experimental test matrix.....	49
Table 4.1 Difference in backfire occurrence near IVO and IVC.....	90
Table 4.2 Summary of effect of parameters on backfire occurrence.....	119
Table 4.3 Summary of effect of parameters on abnormal combustion and remedial measures.....	120

Nomenclatures

Abbreviations

aBDC	after bottom dead center
AMR	adaptive mesh refinement
Ar	argon
aTDC	after top dead center
bBDC	before bottom dead center
BI	backfire intensity
BLER	backfire limiting equivalence ratio
BLIT	backfire limiting injection timing
BLST	backfire limiting spark timing
BON	backfire occurrence number
BP	brake power
bTDC	before top dead center
BTE	brake thermal efficiency
CA	crank angle
CCUS	carbon capture utilization and storage
CFD	computational fluid dynamics

CFL	Courant-Friedrichs-Lewy
COV IMEP	coefficient of variation in indicated mean effective pressure
DC	direct current
ECU	electronic control unit
EGR	exhaust gas recirculation
EGT	exhaust gas temperature
EGT _{critical}	critical exhaust gas temperature
EOC	end of combustion
EVO	exhaust valve opening
FVM	finite volume method
GHG	greenhouse gas
GW	gigawatt
H	hydrogen radical
H ₂	hydrogen
H ₂ O	water
H ₂ O ₂	hydrogen peroxide
HO ₂	hydroperoxyl radical
HRR	heat release rate

Hz	hertz
IC	internal combustion
IL_i	intake valve lift at crank angle i in meters
IL_{max}	maximum intake valve lift in meters
IMEP	indicated mean effective pressure
IVO	intake valve opening
kg	kilogram
kHz	kilohertz
kPa	kilopascal
kW	kilowatt
LBV	laminar burning velocity
μs	microsecond
MBT ST	maximum brake torque spark timing
MJ	megajoule
ms	millisecond
MT	megaton
MW	megawatt
N_2	nitrogen

NO _x	oxides of nitrogen
O	oxygen radical
O ₂	oxygen
OH	hydroxyl radical
PCC	phantom camera control
PMEP	pumping mean effective pressure
ppm	parts per million
RGT	residual gas temperature
RTV	room-temperature-vulcanizing silicone
SD	standard deviation
SE _m	standard error of the mean
SI	spark ignition
SOC	start of combustion
ST	spark timing
TDC	top dead center
TWh	terawatt hour
URANS	unsteady Reynolds Averaged Navier-Stokes
UV	ultraviolet

Symbols

a_c	crank radius (m)
B	bore (m)
CA_{bo}	crank angle location marking backfire origin
CA_{incyl}	crank angle marking a rise in the in-cylinder pressure
CA_{intm}	crank angle marking a rise in the intake manifold pressure
CA_{IVC}	crank angle corresponding to intake valve closing
CA_{SOI}	crank angle corresponding to start of hydrogen injection
C_D	combustion duration
c_p'	specific heat at constant pressure (kJ/kmol K)
c_p	specific heat at constant pressure (kJ/kgK)
c_{pa}	specific heat of air at constant pressure (kJ/kgK)
c_{pch}	specific heat of hydrogen-air charge at constant pressure (kJ/kgK)
c_{pH_2}	specific heat of hydrogen at constant pressure (kJ/kgK)
CV_{H_2}	calorific value of hydrogen (MJ/kg)
$\frac{dA}{d\theta}$	instantaneous surface area of the cylinder (m ²)
$\frac{dp_i}{d\theta}$	rate of pressure rise (bar/degree)

$\frac{dQ}{d\theta}$	gross heat release rate with heat losses (J/degree)
$\frac{dQ_h}{d\theta}$	rate of instantaneous heat transfer (W)
$\frac{dV_i}{d\theta}$	rate of change in cylinder volume (m ³)
h	convective heat transfer coefficient (W/m ² K)
IMEP _n	net indicated mean effective pressure (Pa)
IMEP _{gr}	gross indicated mean effective pressure (Pa)
L	engine stroke (m)
l _c	length of the connecting rod (m)
M	molecular weight (kg/kmol)
\dot{m}_a	mass flow rate of air (kg/s)
m _{a_i}	mass of air at crank angle i in (g/crank angle)
m _{f_i}	mass of hydrogen at crank angle i in (g/crank angle)
\dot{m}_{H_2}	mass flow rate of hydrogen (kg/s)
n	total number of measurements
N	engine speed (rpm)
p	in-cylinder pressure (kPa)
p _i	instantaneous in-cylinder pressure (bar)

$p_i(\theta)$	in-cylinder pressure (Pa)
p_m	motoring pressure of cylinder (bar)
p_r	pressure at the intake valve opening ()
$Q_{c_i}(\theta)$	cumulative heat release at a crank angle (J)
r	engine compression ratio
R	universal gas constant (J/mol K)
R_a	gas constant of air (J/kg K)
R_c	gas constant of hydrogen-air charge (J/kg K)
R_{H_2}	gas constant of hydrogen (J/kg K)
s_{mp}	mean piston speed (m/s)
t	time period of frame (s)
T	reactant temperature (K)
t_{bd}	crank angle between backfire origin and start of hydrogen injection
t_{bo}	time required for the initiation of backfire origin (ms)
t_{bpd}	crank angle difference marking rise in in-cylinder and intake pressure
t_{bps}	backfire propagation time (s)
t_c	cycle time (ms)
T_{exh}	exhaust gas temperature ($^{\circ}$ C)

T_{exh_c}	critical exhaust gas temperature ($^{\circ}\text{C}$)
t_i	induction time (ms)
T_i	intake air temperature ($^{\circ}\text{C}$)
T_{i_g}	in-cylinder mean gas temperature (K)
$T_{i_{g\text{EVO}}}$	in-cylinder mean gas temperature at EVO
t_R	reaction time (ms)
T_r	temperature at intake valve opening (K)
T_{rsg}	residual gas temperature (K)
T_w	average cylinder wall temperature (K)
$V_{\text{avg}_{\text{g}_{\text{bp}}}}$	averaged backfire propagation velocity (m/s)
V_{cc}	cylinder clearance volume (m^3)
V_d	cylinder displaced volume (m^3)
$V_i(\theta)$	instantaneous cylinder volume (m^3)
V_r	volume at intake valve opening
w_{av}	mean gas velocity (m/s)
WD_{gr}	gross indicated work done per cycle (J)
WD_{n}	net indicated work done per cycle (J)
x_{H_2}	mole fraction of hydrogen

y	relative distance between in-cylinder and intake pressure sensor (m)
z_1	distance covered by flame front in the first frame (m)
η_{brake}	brake thermal efficiency (%)
γ	ratio of specific heat of hydrogen-air charge
λ	air-fuel ratio
μ	mean of measurements
μ_{IMEP_n}	mean of measurements of net IMEP
Φ	equivalence ratio
$\frac{\phi}{\text{cycle}}$	equivalence ratio per cycle
ϕ_1	localized equivalence ratio
σ_{IMEP_n}	standard deviation in measurements of net IMEP
τ_{H_2}	induction time of hydrogen
θ_r	crank angle in radians